Pamukkale Üniversitesi Mühendislik Bilimleri Dergisi
Pamukkale University Journal of Engineering Sciences

Kinetic studies of acetophenone derivative oximes and investigation of thermal decomposition mechanism

Asetofenon türevi oksimlerin kinetik çalışmaları ve termal bozunma mekanizmasının incelenmesi

Züleyha Merve İLKİLERİ[1], Emin KARAPINAR[2], Ramazan DONAT[2], Nazan KARAPINAR[1]*

[1]Department of Chemical Engineering, Faculty of Engineering, Pamukkale University, Denizli, Türkiye.
m.ilkileri@gmail.com, nkarapinar@pau.edu.tr
[2]Department of Chemistry, Faculty of Science, Pamukkale University, Denizli, Türkiye.
ekarapinar@pau.edu.tr, rdonat@pau.edu.tr

Received/Geliş Tarihi: 17.01.2025 Revision/Düzeltme Tarihi: 28.02.2025 doi: 10.5505/pajes.2025.35514
Accepted/Kabul Tarihi: 10.03.2025 Research Article/Araştırma Makalesi

Abstract

In this study, two acetophenone derivatives, isonitrosomethyl-p-tolyl ketone (L1) and isonitroso-p-chloroacetophenone (L2), were resynthesized, and their thermal decompositions were investigated kinetically and thermodynamically. Nitrogen gas (5, 10, 15 min flow rate) was used as an inert medium in the thermal decompositions of both ligands. Kinetic analyses were first performed independently of the model using Flynn Wall Ozawa (FWO) and Kissinger Akahira Sunose (KAS) methods, and the effective model in the progression of the reaction was examined by combining the FWO and KAS equations with the model equations together with the graphs of the variation of activation energies with the event fraction. The thermal breakdown processes of L1 and L2 occurred within 25 to 600°C. The effect of heating rate on the TG and DTG curves was studied. As the heating rate went up, so did the temperature needed for the synthetic chemical compounds to break down. The activation energies of the L1molecule, as determined by the KAS and FWO techniques, were 75.96 kJ·mol^{-1} and 79.49 kJ·mol^{-1}, respectively. The computed values for the L2 molecule were 43.80 and 49.37 kJ·mol^{-1}, respectively.

Keywords: Chemical Kinetic, Acetophenone, Thermogravimetry, KAS, FWO

Öz

Bu çalışmada, iki adet asetofenon türevi olan izonitrosometil-p-tolil keton (L1) ve izonitroso-p-kloroasetofenon (L2) ligandları yeniden sentezlenerek kinetik ve termodinamik olarak termal bozunmaları incelenmiştir. Her iki ligandın termal bozunmalarında inert ortam olarak azot gazı (5, 10, 15 dak akış hızı) kullanılmıştır. Kinetik analizler ilk olarak modelden bağımsız olarak Flynn Wall Ozawa (FWO) ve Kissinger Akahira Sunose (KAS) yöntemleri kullanılarak, aktivasyon enerjilerinin olay kesriyle değişiminin grafikleri ile birlikte FWO ve KAS denklemlernini model denklemleriyle birleştirilmiş haliyle reaksiyonun ilerlemesinde etkin model incelenmiştir. İzonitrosometil-p-tolil keton (L1) ve izonitroso-p-kloroasetofenon (L2)'un termal bozunma basamakları 25 ila 600°C arasında gerçekleşti. Isıtma hızının TG ve DTG eğrileri üzerindeki etkisi incelendi. Isıtma hızı arttıkça, sentezlenen kimyasal bileşiklerin parçalanması için gereken sıcaklık da arttı. L1 molekülünün KAS ve FWO teknikleriyle belirlenen aktivasyon enerjileri sırasıyla 75.96 kJ·mol^{-1} ve 79.49 kJ·mol^{-1} idi. L2 molekülü için hesaplanan değerler sırasıyla 43.80 ve 49.37 kJ·mol^{-1} dür.

Anahtar kelimeler: Kimyasal Kinetik, Asetofenon, Termogravimetri, KAS, FWO

1 Introduction

Decomposition is the process by which complex chemical compounds are damaged, destroyed, or broken down into simpler compounds. Thermal decomposition, which results from heat exposure, is a type of decomposition.

The kinetic reaction process is the fundamental part of pyrolysis operations. This reaction process involves mass decomposition, reaction duration, and activation energy [1]. Thermogravimetric analysis (TGA) can comprehensively explain the examination of reaction kinetics in pyrolysis [2]. Mishra et al. assert that the TGA approach for the kinetic analysis of pyrolysis employs exact techniques [3]. It offers quantitative techniques for analyzing the process and identifying an appropriate kinetic parameter. Three primary methodologies exist for ascertaining chemical substances' decomposition kinetics and thermal decomposition characteristics. These encompass thermogravimetry (TG) [4], differential thermogravimetry (DTA) [5], and differential thermogravimetry (DTG) [6].

TGA is a widely used method for investigating the thermal decomposition process and thermal stability of various materials. The data generated by TGA can also determine patterns and parameters of thermal decomposition kinetics.

Kinetics is the study of a chemical reaction's time and temperature dependence. The most common equation used in chemical kinetics is the Arrhenius equation, which the Swedish chemist Svante Arrhenius proposed in 1899. The Arrhenius equation is one of the most important equations in physical chemistry, combining the concept of activation energy and the Boltzmann distribution law.

Based on the above equation, it can be concluded that in order to know the rate constant of a reaction (k), the activation energy (E_a) and the pre-exponential factor (A) are required. E and A are referred to as kinetic parameters. Method of determining or estimating the kinetic parameters.

The kinetic parameters of thermal decomposition have been the subject of several estimation methods. These methods have two basic assumptions: (1) thermal and diffusion differences are eliminated, and (2) the Arrhenius relation is considered valid over the decomposition temperature range. Thermogravimetry (TGA) provides a simple method to determine the thermal decomposition profile and

---

[*] Corresponding author/Yazışılan Yazar

decomposition kinetics of a material. In TGA, only small amounts of material (a few mg) are used so that the boundaries between thermal processes and diffusion processes can be ignored. Based on this, assuming that the Arrhenius relation is valid over the entire temperature range of the thermal decomposition process is reasonable.

In the Arrhenius equation, the decomposition process is assumed to proceed following first-order kinetics (n = 1).

Researchers who study propellant decomposition kinetics want to find the E_a and A values for the Arrhenius equation and how propellant breaks down thermally.

The calculated decomposition kinetics parameters can determine how well propellant ingredients work in the decomposition process and what might happen during it [7].

Thermogravimetry-based instruments, such as the pyrolysis of various chemical compounds, can display thermal decomposition well. The thermal decomposition kinetics of a material can also be determined using thermogravimetric analysis [8]. Two model-independent methodologies, the KAS and FWO approaches, are frequently employed to determine the degradation rates of chemical compounds at elevated temperatures [8]. The KAS and FWO methodologies can be employed to ascertain TG/DTG values. Both methodologies can be used to ascertain the E_a of a pyrolysis process [9,10]. Establishing the activation energy value will yield a thermodynamic assessment of the pyrolysis efficiency of a sample on a broader scale.

In this study, the thermal degradation of isonitrosomethyl-p-tolylketone (L1) and isonitroso-p-chloroacetophenone (L2) synthesized in the thermal analyzer at different heating rates was investigated to determine the change in activation energy according to the degree of conversion. The data obtained from TGA were then analyzed using two independent model methods, KAS and FWO, and activation energy values were determined.

2 Materials and method

2.1 Material

The chemicals used during the study were obtained from companies named Fluka, Merck, and Sigma Aldrich. Sodium metal, butyl nitrite, diethyl ether, ethanol, methanol, acetonitrile, 4-chloro acetophenone, 4-methyl acetophenone acetic acid, P_2O_5, and $CaCl_2$ were used in our experiments. Ethyl alcohol was used during the crystallization processes, and absolute ethyl alcohol was used in the synthesis process. Using these substances, isonitrosomethyl-p-tolylketone (L1) and isonitroso-p-chloroacetophenone (L2) ligands were obtained.

2.2 Synthesis of L1 and L2

Ligands were synthesized similar to the synthesis methods in the literature [11-13].

1.3 g (more than the stoichiometric quantity) of sodium metal was dissolved in 25 mL of absolute ethanol in a glass reactor. 5.85 mL (0.05 mol) of butyl nitrite was slowly added. The mixture was cooled to -15°C and stirred continuously for about 1 hour. At the same temperature, the substance was allowed to stand and stirred for 30 minutes. Add 0.05 mol of 4-methylacetophenone or 0.05 mol of 4-chloracetophenone and stir for about 1 hour. The mixture was stirred for 30 min. and later the mixture was brought to room temperature. The substance, which started to form red crystals, was left to stand for one day. The yellow-red colored substance was washed with 25-30 mL of diethyl ether, and after complete removal of the ether, the substance was thoroughly dissolved with a minimum amount of distilled water. Acetic acid was added to the solution and acidified to a pH of 4.5-5.0. The resulting white solution was filtered and washed several times with distilled water. The precipitate was crystallized in a mixture of 1/2 ethanol and water at 50 to 60°C. The white acicular crystals were dried. Melting point: (L1) 108-110°C, melting point: (L2) 158-160°C (Figure 1 and 2).

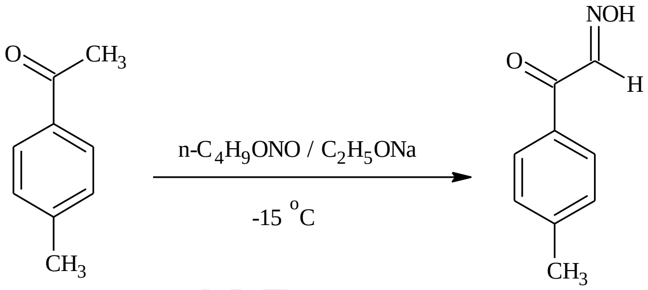

Figure 1. Synthesis reaction of (L1) compound.

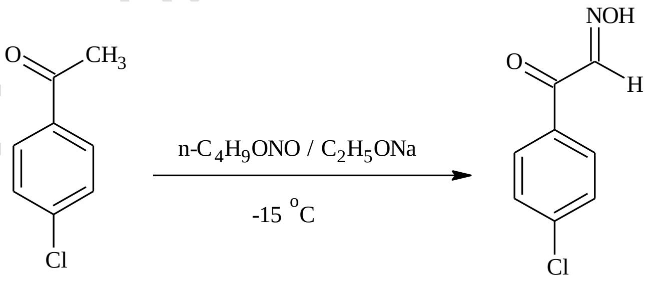

Figure 2. Synthesis reaction of (L2) compound.

2.3 Thermal analysis calculations

The main objective in the evaluation of the data is to use the simplest but most common methods, taking into account the ICTAC-2000 (11th International Congress on Thermal Analysis and Calorimetry) protocol [14,18]. Model-independent approaches are preferred for both differential and integral variables. These methods facilitate the assessment of Arrhenius parameters without needing to select a reaction model. The fundamental aspect of kinetic analysis is understanding the variation in E_a about the degree of conversion (α). This method outlines multi-step procedures and elucidates the response mechanism.

The data obtained in this research is in the form of a curve or thermogram showing the changes in temperature and sample mass. The resulting TG and DTG curves will present the decomposition process of the chemical compounds occurring with each change in the heating rate.

The thermograms were analyzed using two chemical kinetic models, the KAS and FWO methods, to obtain the activation energy values of the chemical compound samples used. A conversion value (α) of 0.1-0.9 is used to determine the activation energy value. The conversion amount α is the ratio of organic matter lost to the total volatile organic matter.

The following equation computes the thermogravimetric analysis of conversion degree [19]:

The reaction rate of a solid is

$$\alpha = \frac{W_o - W_t}{W_o - W_\infty} \tag{1}$$

$$\frac{d\alpha}{dt} = f(\alpha) \tag{2}$$

The formula follows: k represents the rate constant in the Arrhenius equation, while α signifies the fraction of the material that has reacted at time t. f(α) is a function derived from the reaction mechanism.

$$k = A\, exp\left(-\frac{E_a}{RT}\right) \tag{3}$$

Constant heating rate for a non-isothermal system:

It is given as

$$\frac{dT}{dt} = \beta \tag{4}$$

for a non-isothermal system.

From Eq. (2) the following equation is obtained:

$$\frac{d\alpha}{dt} = \left(\frac{d\alpha}{dT}\right)\left(\frac{dT}{dt}\right) = kf(\alpha) \tag{5}$$

When dT/dt in Eq. (4) and k in Eq. (3) are substituted in Eq. (5) and rearranged,

$$\frac{d\alpha}{f(\alpha)} = \frac{A}{\beta}\, exp\left(-\frac{E_a}{RT}\right) dT \tag{6}$$

is obtained. Given that the reaction rate is often minimal at low temperatures, the left and right sides of Eq. (6) may be integrated from 0 to α and from 0 to T, respectively.

$$g(\alpha) = \int_0^\alpha \frac{d\alpha}{f(\alpha)} = \left(\frac{A}{\beta}\right) \int_0^T exp\left(-\frac{E_a}{RT}\right) dT \tag{7}$$

The g(α) is a new function and the expression $\int_0^T exp\left(-\frac{E_a}{RT}\right) dT$ on the right hand side of Eq. (7) is counted the temperature integral. This has no analytical solution.

$x = \frac{E_a}{RT}$ is defined and then $\int_0^T exp\left(-\frac{E_a}{RT}\right) dT$ expression to expression $\frac{E_a}{R} = \int_x^\infty \frac{e^{-x}}{x^2} dx = \left(\frac{E}{R}\right) P(x)$ is converted. P(x) is an infinite function of x. Thus, by substituting the temperature integral value in Eq. (7), the following expression is obtained:

$$g(\alpha) = \int_0^\alpha \frac{d\alpha}{f(\alpha)} = \frac{E_a A P(x)}{R\beta} \tag{8}$$

Since the value of E_a/R is constant, the value of $\int_0^\alpha \frac{d\alpha}{f(\alpha)}$ depends on the value of the function P(x). Doyle evaluates the P(x) function and suggests that P(x) is log P(x)=-2.315-0.4567x in the range x 20 ≤ x ≤ 60 [20].

2.3.1 Kissinger–Akahira–Sunose (KAS) method

The KAS method is an iso-conversion technique used to derive the kinetics of solid-state reactions without requiring knowledge of the reaction mechanism. Kissinger established it in 1956, allowing for the derivation of the variation of peak temperature with heating rate from the kinetics of the reaction in differential thermal analysis. The KAS method is an integral method in which the E_a can be determined for the conversion (α) values without knowing the reaction order. KAS method [21, 22] is based on taking the differential of Eq. (6). According to this,

$$\ln\frac{\beta}{T^2} = \ln\left[\frac{AR}{T}\right] - \frac{E_a}{RT} + \frac{df(\alpha)}{d\alpha} \tag{9}$$

is obtained. The activation energy for each α at constant heating rate is calculated from the slope of the ln $\beta/T2$ versus $1/T$ plot.

2.3.2 Flynn–Wall–Ozawa (FWO) method

Ozawa and Flynn-Wall independently developed the FWO method, another integral method for computing non-isothermal data [23, 24]. The Doyle approach, along with the logarithmic form of Equation (7), yields the linear equation of the FWO method [20]:

$$\log(\beta) = log\left(\frac{AE}{g(\alpha)R}\right) - 2.315 - 0.457\left(\frac{E_a}{RT}\right) \tag{10}$$

By converting the logarithmic expression to natural logarithm (ln), Eq. (10) can be rewritten.

$$\ln(\beta) = ln\left(\frac{AE}{g(\alpha)R}\right) - 5.331 - 1.052\left(\frac{E_a}{RT}\right) \tag{11}$$

Activation energies are calculated from the slopes of the ln β versus 1/T plots, considering the same conversion (α) of the reaction for different heating rates. In the study, activation energies were obtained and compared with both methods.

2.4 Prediction of g(α) reaction mechanism

The methods proposed by Ortega predict the mechanism of the reactions [25]. The average of the activation energies obtained by the KAS and FWO methods is used to find the reaction mechanism. Eq.(12) is obtained by rearranging Equation (11).

$$\ln(g(\alpha)) = ln\left(\frac{AE}{\beta R}\right) - 5.331 - 1.052\left(\frac{E}{RT}\right) \tag{12}$$

Several solid-state mechanisms' activation energies are compared to the average activation energy from FWO. The mechanism whose activation energy is closest to this value is then chosen. Subsequently, with the mechanism established, the ln(A) value is computed by substituting the activation energy into Equation (12).

The rate-determining steps in solid-state reactions are diffusion and chemical reaction. An average behavior that addresses both steps, or transition states between the two, can be used. Transitional states are based on the following assumptions: The first assumption is initial surface diffusion. The continuously developing product layer rapidly envelops the reactant's surface. The second assumption addresses the nucleation of products at active sites and the growth rate of the nucleated particles. In this context, kinetic functions are categorized into three kinds: diffusion, chemical reaction, and nucleation [26].

Nucleation (An) can be defined as the formation of a new and different product in a solid reactant. Transformation of the reactant into product components and recrystallization of the reacted substance in the lattice structure of the product phase can occur. Nucleation, which perhaps requires several steps, occurs as the nucleus grows. It occurs at the active reactant-product interface, where the reaction occurs by progressing into the reactant [27]. If particle nucleation occurs randomly, such a kinetic behavior can be observed in the degradation of powders. Growth then does not proceed in a nucleated single crystal [26].

3 Results and Discussion

3.1 Thermal analysis of ligands

The TG and DTG curves of isonitrosomethyl-p-tolyl ketone and isonitroso-p-chloroacetophenone compounds obtained at heating rates of 5, 10, and 15^{o}C min^{-1} in a nitrogen atmosphere are given in Figures 3-6, respectively. As shown from the figures of both compounds' TG and DTG curves, the sample decomposes at approximately 150^{o}C, and the decomposition temperature increases with an increasing heating rate. At low heating rates, a significant increase in the system's thermal energy occurs, and a long time is required for the temperature of the sample to come into balance with the temperature of the furnace. The reaction time decreases at elevated heating rates for the same duration and within the identical temperature range. Consequently, the temperature necessary for the sample's decomposition is elevated, resulting in an upward displacement of the maximum speed curve.

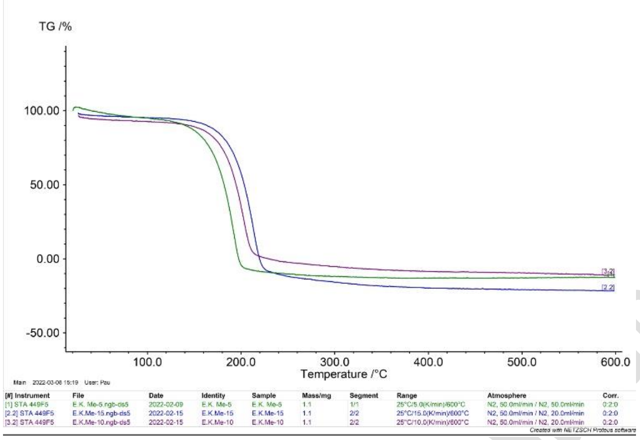

Figure 3. DTG curves of isonitrosomethyl-p-tolylketone ligand at different heating rates.

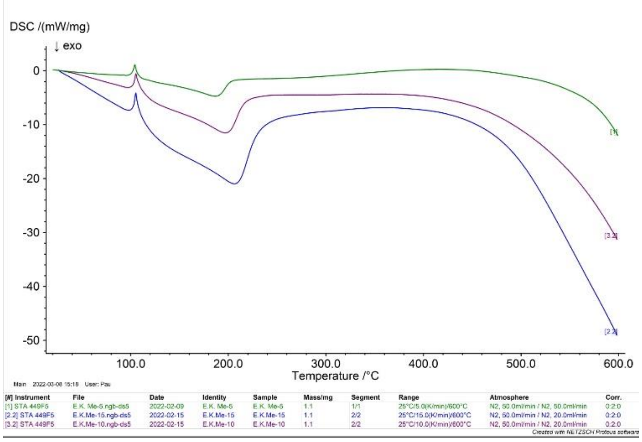

Figure 4. DSC curves of isonitrosomethyl-p-tolylketone ligand at different heating rates.

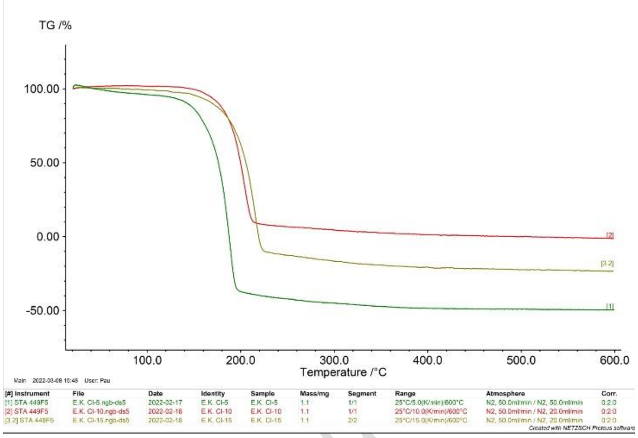

Figure 5. DTG curves of isonitroso-p-chloroacetophenone ligand at different heating rates.

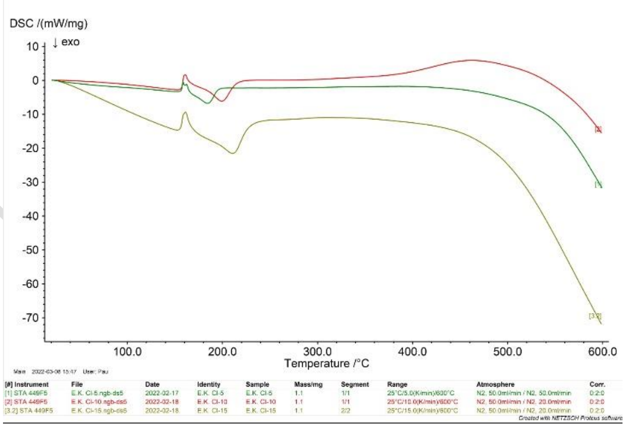

Figure 6. DSC curves of isonitroso-p-chloroacetophenone ligand at different heating rates.

3.2 Effects of heating rate

TDTG$_{max}$ ranges from 195 to 229 and 218°C for heating rates of 5, 10, and 15°C min^{-1}. The isonitrosomethyl-p-tolylketone ligand degredation in TG curves in a nitrogen atmosphere. The TDTG$_{max}$ of *B* in N$_2$ ranges from 185 to 490 and 217°C, respectively, at identical heating rates (Table 1).

This study aimed at Tp of the iso nitroso-p-chloroacetophenone ligand at 40, 26, and 26 °C with heating rates of 5, 10, and 15 °C min-1 in a N$_2$ atmosphere (Figure 3 and Table 1). Under N$_2$ atmosphere, the iso nitroso-p-chloroacetophenone ligand raises Tp from 185°C to 490°C and 74°C, at steady heating rates (see Figure 5 and Table 1), respectively.

According to these results, TG-DSC curves tend to increase to higher temperatures with increasing heating rates. The different analysis times cause TG$_{max}$ and Tp to be different. However, considering the places where the mass loss decreases significantly and the end of the loss starts and ends, a relative increase in Tp was observed at the same temperatures where

Table 1. Active temperature range of isonitrosomethyl-p-tolylketone and isonitroso-p-chloroacetophenone ligand pyrolysis at each heating rate obtained by TG at different scanning speeds and in the N$_2$ atmosphere.

Ligand type	Decom. step	Heating rate (°C/min)	Starting Temperature T_{onset} (°C)	DTGmax. temperature $T_{DTGmax.}$ (°C)	Final temperature T_{endset} (°C)
L1	1	5	40	195	598
		10	26	229	596
		15	26	218	596
L2	1	5	45	185	598
		10	148	490	598
		15	74	217	597

T_{DTGmax} increases. With the increase in heating rate, the system has a resistive and retarding effect on the decomposition since it has less time to "respond" to the temperature change.

Under the N_2 atmosphere, the Tp of the isonitrosomethyl-p-tolyl ketone ligand was determined to be 40, 26, and 26 under the same conditions (Figure 3 and Table 1). At the same heating rates, the Tp of isonitroso-p-chloroacetophenone in N_2 increased from 185 to 490 and 74°C (Figure 5 and Table 1). According to these results, TG-DSC curves tended to shift towards higher temperatures with increasing heating rates. TG_{max} and Tp are not regular because the analysis was done at different times, and the same standard could not be reached. In addition, when the areas where the significant decrease in mass loss started and ended were examined, it was seen that T_{DTGmax} increased with the expansion of the temperature range and heating rates; similarly, a higher-than-expected Tp increase was seen. Since the system's response time to the temperature change decreases in response to the increasing heating rate, it exerts a resistant and inhibitory effect on the separation.

3.3 Kinetic analyses

To find out how kinetic parameters affect conversion (α), the thermogravimetric investigation is used for the investigation of weight loss curves recorded at different heating rates. The compound bioconversion values for isonitrosomethyl-p-tolylketone and isonitroso-p-chloroacetophenone were derived from thermogravimetric data at each temperature increment.

The FWO and KAS methodologies were used to compute the kinetic parameters. We found the ln (β/T^2) vs. $1000/T$ for isonitrosomethyl-p-tolylketone and isonitroso-p-chloroacetophenone conversion rates with α ranging from 0.1 to 0.9 via both the KAS method on Eq. 9. They are shown in both Figure 7 and 8. The activation energies were derived from the slope of the resulting lines.

Furthermore, E_a were determined using the FWO approach as outlined in Eq. 10. The graphs of ln β vs. $1/T$ for various transformations are presented in Figures 9 and 10, and the activation energies are derived from the slopes of the resulting lines. The slopes are equivalent to -E_a/R. The lines from the KAS and FWO methods are almost parallel, as shown in Figures 7 and 9. The changes in activation energies found by using the conversion fraction are also similar. The discrepancies noted between E_a values derived from linear integration methods can be attributed to varying approaches to temperature integration. The activation energies (E_a) and correlation coefficients (R^2) determined using both methods are presented in Table 2.

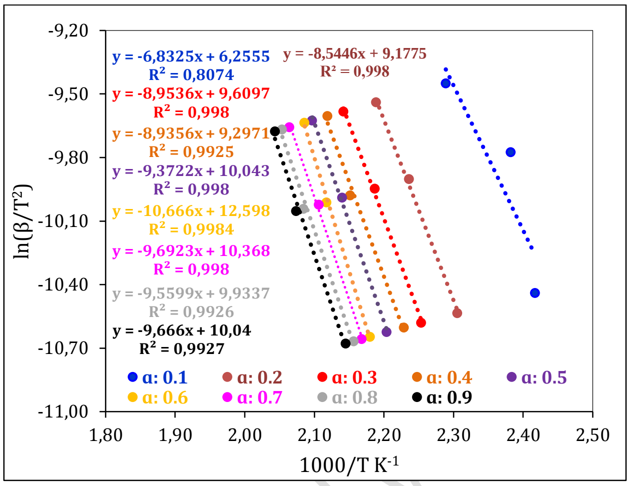

Figure 7. Plot of ln(β/T^2) versus 1000/K^{-1} of L1 ligand in N_2 atmospheres according to KAS.

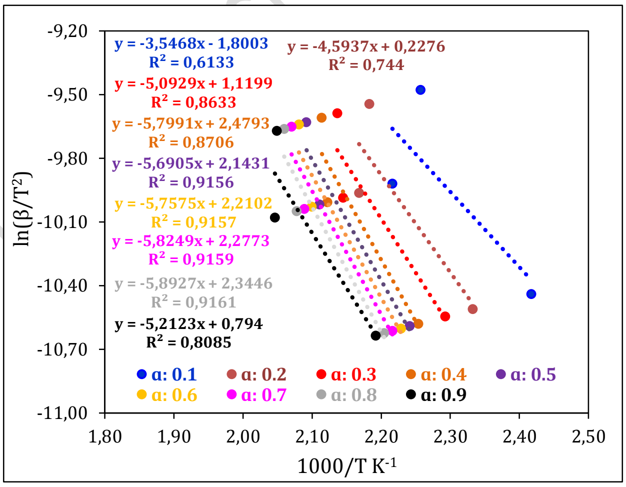

Figure 8. Plot of ln(β/T^2) versus 1000/K^{-1} of L2 ligand in N_2 atmospheres according to KAS.

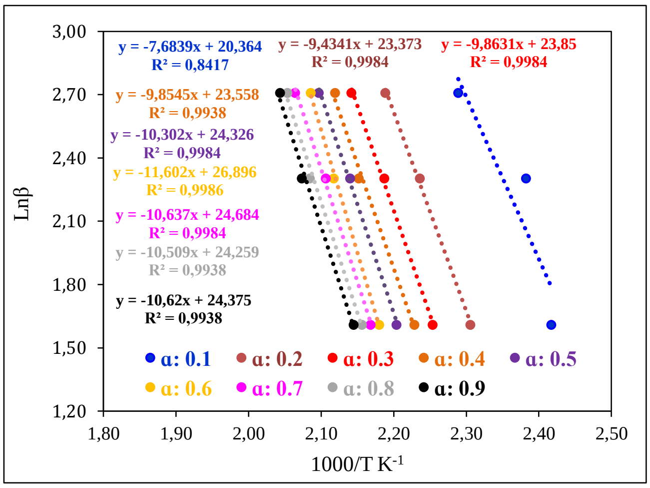

Figure 9. Plot of lnβ versus 1000/K^{-1} L1 ligand in N_2 atmospheres according to FWO

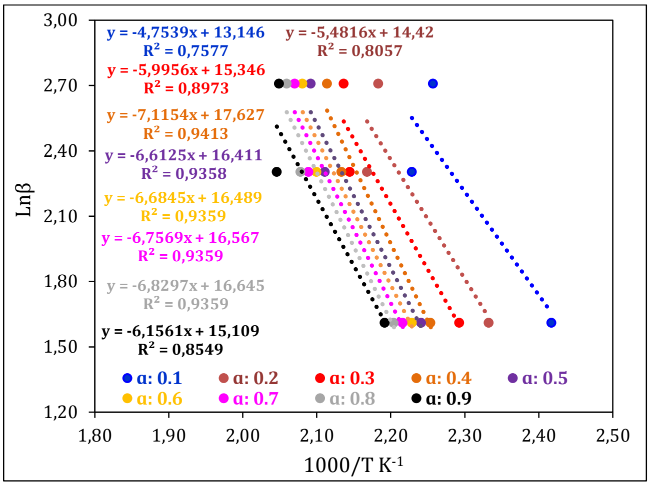

Figure 10. Plot of lnβ versus 1000/K^{-1} of and L2 ligand in N_2 atmospheres according to FWO.

Table 2. E_a values of thermal decomposition steps Isonitrosomethyl-p-tolylketone ligand (L1) and isonitroso-p-chloroacetophenone(L2) from FWO and KAS methods in N_2 atmospheres.

Ligand	α	FWO E_a/(kJ·mol^{-1})	R^2	KAS E_a/(kJ·mol^{-1})	R^2
L1	0.1	60.74	0.8417	56.81	0.8074
	0.2	74.57	0.9984	71.04	0.998
	0.3	77.97	0.9984	74.44	0.998
	0.4	77.90	0.9938	74.29	0.9925
	0.5	81.43	0.9984	77.92	0.998
	0.6	91.71	0.9986	88.68	0.9984
	0.7	84.08	0.9984	80.58	0.998
	0.8	83.07	0.9938	79.48	0.9926
	0.9	83.95	0.9938	80.37	0.9927
	Ave.	79.49		75.96	
L2	0.1	37.58	0.7577	29.49	0.6133
	0.2	43.33	0.8057	38.19	0.744
	0.3	47.39	0.8973	42.34	0.8633
	0.4	56.25	0.9413	48.21	0.8706
	0.5	52.27	0.9358	47.31	0.9156
	0.6	52.84	0.9359	47.87	0.9157
	0.7	51.99	0.9359	48.43	0.9159
	0.8	53.99	0.9359	48.99	0.9161
	0.9	48.66	0.8549	43.34	0.8085
	Ave.	49.37		43.80	

The average activation energy for isonitrosomethyl-p-tolylketone was found to be 75.96 kJ·mol^{-1} using the KAS method and 79.49 kJ·mol^{-1} using the FWO method (as shown in Table 2). The average activation energies for isonitroso-p-chloroacetophenone, determined by the KAS and FWO techniques, were calculated to be 43.80 kJ mol^{-1} and 49.37 kJ·mol^{-1}, respectively.

It can be seen from Table 2 that the E_a values obtained from the FWO and KAS methods for both compounds are close to each other. This is due to the fact that the FWO and KAS methods are nonisothermal. The World Confederation of Thermal Analysis and Calorimetry (ICTAC) announced at its 2000 traditional meeting that nonisothermal methods are more suitable, reliable, and reproducible in thermokinetic analysis and that nonisothermal methods should be used in thermokinetic analysis [28]. For this reason, FWO and KAS results should be taken into account.

The presence of methyl in ligand isonitrosomethyl-p-tolylketone and chlorine in Ligand isonitroso-p-chloroacetophenone increases the electronegativity of the ligand because the chlorine atom attached to the ligand increases the electronegativity of the ligand, pulling electrons from the ligand to such an extent that thermal separation of fragments from the ligand becomes difficult. In this case, the Ea activation energy of the E_a thermal reaction also increases [29].

3.4 Reaction order and activation energy of isonitrosomethyl-p-tolylketone and isonitroso-p-chloroacetophenone

Using thermal analysis data for isonitrosomethyl-p-tolylketone and isonitroso-p-chloroacetophenone at varying temperature ranges and rates (5, 10, and 15°C min^{-1}), the kinetics of degradation and activation energies of the reaction were calculated and the values found are given in Tables 3 and 4, respectively.

4 Conclusion

This study investigates the kinetics of isonitrosomethyl-p-tolylketone and isonitroso-p-chloroacetophenone. The mass fractionation of the reaction was ascertained utilizing the DTA, TG, and DTG curves. A model-independent method was used to do the kinetic analysis to find out the reaction's kinetic parameters based on the results of the thermogravimetric study. The activation energy (E_a) and the preexponential component (A) were ascertained utilizing the KAS and FWO methodologies.

Thermogravimetric and kinetic studies of the two compounds were conducted in a nitrogen environment at varying heating rates of 5°C·min^{-1}, 10°C·min^{-1}, and 15°C·min^{-1}. The thermal breakdown processes of isonitrosomethyl-p-tolyl ketone and isonitroso-p-chloroacetophenone occurred within 25 to 600°C. The effect of heating rate on the TG and DTG curves was studied. As the heating rate went up, so did the temperature needed for the synthetic chemical compounds to break down. The activation energies of the isonitrosomethyl-p-tolyl ketone molecule, as determined by the KAS and FWO techniques, were 75.96 kJ·mol^{-1} and 79.49 kJ·mol^{-1}, respectively. The computed values for the iso nitroso-p-chloroacetophenone molecule were 43.80 and 49.37 kJ·mol^{-1}, respectively. Apparent average values were employed for the activation energies derived from KAS and FWO.

From the experimental results, it can be concluded that the model-free approach is successful in describing the complexity of the pyrolysis process.

.

Table 3. Reaction step and activation energy values for the degradation of isonitrosomethyl-p-tolylketone compound at varying temperature ranges and rates.

	β = 5^{o}C/min^{-1}			β =10^{o}C/min^{-1}			β =15^{o}C/min^{-1}		
Order	Temp. Range (^{o}C)	E_a (kJ·mol^{-1})	R^2	Temp. Range (^{o}C)	E_a (kJ·mol^{-1})	R^2	Temp. Range (^{o}C)	E_a (kJ·mol^{-1})	R^2
n=1	45.53-65.53	46.51	0.9529	23.05-38.05	8.65	0.8663	33.71-48.71	4.78	0.9356
	63.03-120.53	9.29	0.9706	40.55-120.55	-1.34	0.92	133.71-156.21	17.55	0.978
	123.03-135.53	22.92	0.9986	123.05-143.05	9.38	0.966	158.71-181.21	50.34	0.9908
	140.53-158.03	50.31	0.9944	145.55-170.55	39.76	0.9766	183.71-213.71	98.80	0.9927
	160.53-178.03	95.79	0.9881	175.55-203.05	121.98	0.9834			
n=1/3	45.53-65.53	45.99	0.9522	205.55-223.05	42.98	0.9869	33.71-48.71	4.66	0.9339
	63.03-120.53	8.90	0.9689	23.05-38.05	8.41	0.8633	133.71-156.21	16.95	0.978
	123.03-135.53	21.61	0.9986	40.55-120.55	-1.45	0.9343	158.71-181.21	47.63	0.9918
	140.53-158.03	45.59	0.9955	123.05-143.05	-8.83	0.965	183.71-213.71	82.92	0.9972
	160.53-178.03	73.21	0.9957	145.55-170.55	37.00	0.9782			
				175.55-203.05	85.48	0.9982			
n=1/2	45.53-65.53	46.14	0.9524	23.059-38.05	8.48	0.8642	33.71-48.71	4.70	0.9344
	63.03-120.53	9.01	0.9684	40.559-120.55	-1.42	0.9306	133.71-156.21	17.12	0.978
	123.03-135.53	21.98	0.9986	123.05-143.05	8.99	0.9653	158.71-181.21	48.39	0.9915
	140.53-158.03	46.91	0.9952	145.55-170.55	37.78	0.9778	183.71-213.71	87.26	0.9961
	160.53-178.03	79.23	0.9938	175.55-203.05	121.98	0.9834			
n=2/3	45.53-65.53	46.26	0.9525	23.05-38.05	38.43	0.9774	33.71-48.71	4.72	0.9348
	63.03-120.53	9.10	0.9698	40.55-120.55	-1.39	0.9273	133.71-156.21	17.26	0.978
	123.03-135.53	22.29	0.9986	123.05-143.05	9.12	0.9656	158.71-181.21	49.03	0.9913
	140.53-158.03	48.02	0.9949	145.55-170.55	38.43	0.9774	183.71-213.71	91.00	0.9951
	160.53-178.03	84.51	0.992	175.55-203.05	103.21	0.9927			
n=2	45.53-65.53	47.25	0.9538	23.05-38.05	8.65	0.8663	33.71-48.71	4.94	0.9379
	63.03-120.53	9.86	0.9726	40.55-120.55	-1.18	0.8916	133.71-156.21	18.43	0.9779
	123.03-135.53	24.85	0.9985	123.05-143.05	10.19	0.9673	158.71-181.21	54.36	0.9893
	140.53-158.03	57.54	0.9922	145.55-170.55	43.90	0.9743	183.71-213.71	124.91	0.9841
	160.53-178.03	135.38	0.9749	175.55-203.05	193.49	0.9429			

Table 4. Reaction step and activation energy values in the degradation of isonitroso-p-chloroacetophenone compound at varying temperature ranges and rates.

	5°C/min^{-1}			10°C/min^{-1}			15°C/min^{-1}		
Order	Temp. Range (°C)	E_a (kJ·mol^{-1})	R^2	Temp. Range (°C)	E_a (kJ·mol^{-1})	R^2	Temp. Range (°C)	E_a (kJ·mol^{-1})	R^2
n=1	45.52-55.52	146.28	0.9827	155.559-213.05	138.21	0.9941	82.373-14.87	41.438	0.9680
	60.52-75.52	26.22	0.9781	218.059-295.55	-2.30	0.9355	147.37-192.37	65.761	0.9976
	78.02-110.52	11.35	0.9943	298.059-483.05	3.17	0.4423			
	113.02-138.02	25.08	0.9731						
	145.52-175.52	84.58	0.9946						
n=1/3	45.52-55.52	145.97	0.9826	155.55-213.05	121.57	0.9954	82.37-144.87	41.231	0.9676
	60.52-75.52	25.95	0.9778	218.05-295.55	-6.66	0.9977	147.37-192.37	62.77	0.9987
	78.02-110.52	11.1	0.9942	298.05-483.05	-8.77	0.9965			
	113.02-138.02	24.3	0.9735						
	145.52-175.52	74.1	0.9981						
n=1/2	45.52-55.52	146.06	0.9826	155.55-213.05	125.97	0.9963	82.37-144.87	41.29	0.9677
	60.52-75.52	26.03	0.9979	218.05-295.55	-5.77	0.996	147.37-192.37	63.614	0.9984
	78.02-110.52	11.17	0.9942	298.05-483.05	-7.01	0.9938			
	113.02-138.02	24.52	0.9734						
	145.52-175.52	76.99	0.9973						
n=2/3	45.524-55.52	146.14	0.9826	155.55-213.05	129.85	0.9964	82.37-144.87	41.34	0.9678
	60.52-75.52	26.09	0.9780	218.05-295.55	-4.83	0.9923	147.37-192.37	64.324	0.9982
	78.02-110.52	11.23	0.9942	298.05-483.05	-4.60	0.9325			
	113.02-138.02	24.71	0.9733						
	145.52-175.52	79.46	0.9965						
n=2	45.52-55.52	146.73	0.9829	155.55-213.059	168.16	0.9682	82.37-144.87	41.735	0.9685
	60.52-75.52	26.6	0.9784	218.05-295.559	10.28	0.9716	147.37-192.37	70.215	0.9957
	78.02-110.52	11.72	0.9944	298.05-483.059	53.31	0.8143			
	113.02-138.02	26.21	0.9726						
	145.52-175.52	101.37	0.9868						

5 Acknowledgements

This study was supported by Scientific Research Coordination Unit of Pamukkale University under the project Number 2021FEBE030.

6 Author contribution statements

In the study carried out, Author 1 contributed to the re-synthesis of the substances, data collection, software and literature review of the data; Author 2 contributed to the re-synthesis of the substances, the writing of the draft article, checking the article in terms of content and Author 3 contributed to the writing of the draft article, creation of figures and tables, checking the article in terms of content and evaluation of the results; Author 4 contributed to the formation of the idea, the design of the experiments and evaluation of the obtained results.

7 Ethics committee approval and conflict of interest statement

“There is no need to obtain permission from the ethics committee for the article prepared”. “There is no conflict of interest with any person/institution in the article prepared”.

8 References

[1] Chen R, Zhang D, Xu X, Yuan Y. “Pyrolysis characteristics, kinetics, thermodynamics and volatile products of waste medical surgical mask rope by thermogravimetry and online thermogravimetry-Fourier transform infrared-mass spectrometry analysis”. *Fuel,* 295,120632, 2021.

[2] Saeed S, Ashour I, Sherif H, Ali MRO. “Catalytic and noncatalytic fast pyrolysis of jatropha seeds: Experimental measurements and modeling”. *Egyptian Journal of Chemistry*, 63, 683–702, 2020.

[3] Mishra G, Kumar J, Bhaskar T. “Kinetic studies on the pyrolysis of pinewood”. *Bioresource Technolgy*, 182, 282–288, 2015.

[4] Singh S, Patil T, Tekade SP, Gawande MB, Sawarkar AN. “Studies on individual pyrolysis and co-pyrolysis of corn cob and polyethylene: Thermal degradation behavior, possible synergism, kinetics, and thermodynamic analysis”. *The Science of The Total Environment*, 783, 147004, 2021.

[5] Wen Y, Wang S, Mu W, Yang W, Jönsson PG. “Pyrolysis performance of peat moss: A simultaneous in-situ thermal analysis and bench-scale experimental study”. Fuel, 277, 118173, 2020.

[6] Wang X, Hu M, Hu W, Chen Z, Liu S, Hu Z, Xiao B. “Thermogravimetric kinetic study of agricultural residue biomass pyrolysis based on combined kinetics”. *Bioresource Technolgy*. 219, 510–520, 2016.

[7] Vargeese, Anuj A. "A Kinetics Investigationon The Mechanism and Activity of CopperOxide Nanorods on The Thermal Decomposition of Propellants”. *Combustion and Flame*, 165, 354-360, 2016.

[8] Dewi, W.U. “Evaluasi Kinetika Dekomposisi Termal Propelan Komposit Ap/Htpb Dengan Metode Kissinger, Flynn Wall Ozawa Dan Coats - Redfren (Evaluation of Thermal Decomposition Kinetics of Ap/Htpb Composite Solid Propellant Using Kissinger, Flynn Wall Ozawa and Coats”. *Jurnal Teknologi Dirgantara*, 15, 115–32, 2017.

[9] Mothe´ CG, de Miranda I.C. “Study of kinetic parameters of thermal decomposition of bagasse and sugarcane straw using Friedman and Ozawa–Flynn– Wall isoconversional methods”. *Journal of Thermal Analysis and Calorimetry*, 113(2), 497–505, 2013.

[10] Rego F, Dias APS, Casquilho M, Rosa F C, Rodrigues, A. “Pyrolysis kinetics of short rotation coppice poplar biomass”. *Energy*, 207, 118191, 2020.

[11] Pekacar Aİ. Synthesis of Different Phenylglyoximes Containing Different Substituted Amine Groups and Investigation of Their Metal Complexes. PhD Thesis, Selcuk University, Konya, Turkey, 1994.

[12] Sevindir HC. Synthesis of vic-Dioximes Containing Different Substituents and Investigation of Some Transition Metal Complexes of Them. PhD Thesis, Selcuk University, Konya, Turkey, 1992.

[13] Karapınar E, Karapınar N, Özcan E. “Synthesis of N’-(4’-benzo[15-crown-5])phenylaminoglyoxime and its Complexes with Nickel(II), Cobalt(II) and Copper(II)”. *Synthesis and Reactivity in Inorganic and Metal-Organic Chemistry*, 33(8), 1319-1328, 2003.

[14] Brown ME, Maciejewski M, Vyazovkin S, Nomen R, Sempere J, Burnham A, Opfermann J, Strey R, Anderson HL, Kemmler A, Keuleers R, Janssens J, Desseyn HO, Li Chao-Rui, Tang, Tong B, Roduit B, Malek J, Mitsuhashi T. “Computational Aspects of Kinetic Analysis: Part A: The ICTAC Kinetics Project-Data, Methods and Results”. *Thermochimica Acta*, 355(1-2), 125-143, 2000.

[15] Maciejewski M. “Computational Aspects of Kinetic Analysis. Part B: The ICTAC Kinetics Project-The Decomposition Kinetics of Calcium Carbonate Revisited, or Some Tips on Survival in the Kinetic Minefield”. *Thermochimica Acta*, 355(1-2), 145-154, 2000.

[16] Vyazovkin S. “Computational Aspects of Kinetic Analysis. Part C. The ICTAC Kinetics Project-The Light at the End of the Tunnel”. *Thermochimica Acta*, 355(1-2), 155-163, 2000.

[17] Burnham AK. “Computational Aspects of Kinetic Analysis. Part D: The ICTAC Kinetics Project-Multi-Thermal-History Model-Fitting Methods and Their Relation to Isoconversional Methods”. *Thermochimica Acta*, 355(1-2), 165-170, 2000.

[18] Roduit B. “Computational Aspects of Kinetic Analysis. Part E: The ICTAC Kinetics Project-Numerical Techniques and Kinetics of Solid State Processes”. *Thermochimica Acta*, 355(1-2), 171-180, 2000.

[19] Morancho JM, Salla JM, Cadenato A. Fernández-Francos X, Ramis X, Colomer P, Calventus Y, Ruíz R. ‘‘Kinetic Studies of the Degradation of Poly(vinyl alcohol)-Based ProtonConducting Membranes at Low Temperatures’’. *Thermochimica Acta*, 521(1-2), 139-147, 2011.

[20] Doyle CD. “Estimating Isothermal Life From Thermogravimetric Data”. *Journal of Applied Polymer Science*, 6(24), 639-642, 1962.

[21] Kissinger H. “Variation of Peak Temperature With Heating Rate in Differential Thermal Analysis”. *Journal of Research of the National Bureau of Standards*, 57(4), 217-221, 1956.

[22] Akahira T, Sunose T. “Joint Convention of Four Electrical Institutes”. *Science Technology*, 16, 22–31, 1971.

[23] Ozawa T. “A New Method of Analyzing Thermogravimetric Data”. *Bulletin of the Chemical Society of Japan*, 38(11), 1881-1886, 1965.

[24] Flynn J, Wall L. “A Quick, Direct Method for the Determination of Activation Energy from Thermogravimetric Data”. *Journal of Polymer Science Part B: Polymer Letters*, 4(5), 323-328, 1966.

[25] Ortega A. “Some Successes and Failures of the Methods Based on Several Experiments”. *Thermochima Acta*, 284(2), 379–387, 1996.

[26] Halikia I, Zoumpoulakis L, Christodoulou E, Prattis D. “Kinetic Study of the Thermal Decomposition of Calcium Carbonate by Isothermal Methods of Analysis”. *The European Journal of Mineral Processing and Environmental Protection*, 1(2), 89-102, 2001.

[27] Galwey AK, Brown ME. *Kinetic Background to Thermal Analysis and Calorimetry*. Editor: Brown ME. Handbook of Thermal Analysis and Calorimetry Principles and Practice, 691, Amsterdam, Holland, Elsevier Scientific, 1998.

[28] Vyazovkin S, Burnham AK, Criado JM, Perez-Maqueda LA., Popescu C, Sbirazzuoli N, “ICTAC Kinetics Committee recommendations for performing kinetic computations on thermal analysis data”. *Thermochim. Acta*. 520:1-19, 2011.

[29] Tuncer YG. Investigation of Coordination Compounds Prepared Using Bis(N,N’-Salicylidene)-1,3-Diaminopropane Ligand and Heterocyclic Compounds by Thermal Analysis Methods. MSc Thesis, Ankara University, Ankara, Turkey, 2021.